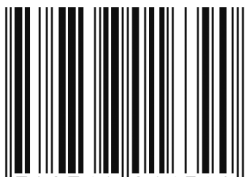

Surge Definitions for Radial Compressors in Automotive Turbochargers

Johannes Andersen, Fredrik Lindström and Fredrik Westin
GM Powertrain Sweden AB

ISBN 978-0-7680-1639-0



9 780768 016390

SAE *International*[™]

**2008 World Congress
Detroit, Michigan
April 14-17, 2008**

By mandate of the Engineering Meetings Board, this paper has been approved for SAE publication upon completion of a peer review process by a minimum of three (3) industry experts under the supervision of the session organizer.

All rights reserved. No part of this publication may be reproduced, stored in a retrieval system, or transmitted, in any form or by any means, electronic, mechanical, photocopying, recording, or otherwise, without the prior written permission of SAE.

For permission and licensing requests contact:

SAE Permissions
400 Commonwealth Drive
Warrendale, PA 15096-0001-USA
Email: permissions@sae.org
Tel: 724-772-4028
Fax: 724-776-3036



For multiple print copies contact:

SAE Customer Service
Tel: 877-606-7323 (inside USA and Canada)
Tel: 724-776-4970 (outside USA)
Fax: 724-776-0790
Email: CustomerService@sae.org

ISSN 0148-7191

Copyright © 2008 SAE International

Positions and opinions advanced in this paper are those of the author(s) and not necessarily those of SAE. The author is solely responsible for the content of the paper. A process is available by which discussions will be printed with the paper if it is published in SAE Transactions.

Persons wishing to submit papers to be considered for presentation or publication by SAE should send the manuscript or a 300 word abstract of a proposed manuscript to: Secretary, Engineering Meetings Board, SAE.

Printed in USA

Surge Definitions for Radial Compressors in Automotive Turbochargers

Johannes Andersen, Fredrik Lindström and Fredrik Westin

GM Powertrain Sweden AB

Copyright © 2008 SAE International

ABSTRACT

A standardized measurement setup and definition of compressor surge is yet to be established in the automotive community. As a consequence, compressor comparisons with regards to compressor operating map width is practically impossible today. This paper presents a possible solution to the described problem by presenting a suitable instrumentation and a correlation between measured values and actual NVH limits normally encountered in turbocharged vehicle applications. The work has been performed in laboratory conditions in a compressor test rig with both steady and pulsating flow as well as in a gas stand with steady flow. The test rig design, measurement setup and error sources are described. Some effects of different boundary conditions to the compressor and how they affect the measurement method are also presented. The definitions and viability of the described methods have been validated through vehicle tests to ensure the possibility of application not only in lab environment but also in actual field use.

INTRODUCTION

The process of developing new powertrain solutions is more and more time constrained. This triggers methods that can form the basis of good engineering decisions very early on in the projects. These methods must in most cases be independent on hardware availability, and thus simulations and single component testing have been given a larger role in engine development. In the case of simulating and predicting turbocharged engines there is a significant dependency on correct data input in the form of compressor and turbine maps.

The compressor map is limited at low flow rates by flow instability known as surge and at higher flow rates by choke. There are numerous methods for measuring and quantifying the surge region, some of which are presented in this paper, but there has to this date not surfaced any correlation between these indicators and the actual vehicle NVH limits. Evidently, there is a need for obtaining data that can give simulation engineers real limits in the compressor map data that fulfills the NVH requirements.

SURGE IN RADIAL COMPRESSOR - A radial compressor used in automotive turbochargers can be divided in four main components:

- The inducer, where the air is accelerated, into the impeller
- The impeller, in which there are acceleration and diffusion to various extent depending on design
- The diffuser, which is the part of the compressor that is primarily designed for diffusion, i.e. transforming dynamic pressure to static pressure
- The volute, which collects the air from the diffuser and transports the air out of the compressor and in which there normally is diffusion to a certain extent

The phenomenon of compressor surge is basically a problem of air stalling which leads to flow reversal and recirculation within the compressor, which can result in either a local instability and sound problems or complete compressor instability and unacceptable drivability issues in a vehicle. The stalling of air is likely to occur when air flow is low and the pressure gradient is too high for the inertia of the gas to withstand a reverse in flow, and therefore the surge limit is the leftmost border in any compressor map.

Local stall or flow reversal in a component will cause a reduction in efficiency or pressure build-up but does not necessarily lead to complete compressor system instability and surge. Stable operation with inducer stall is possible at low pressure ratios and is accompanied with a local temperature rise in the compressor inlet. At higher pressure ratios or compressor speeds, inducer stall invariably leads to surge according to previous research [1][2].

SURGE ON TURBOCHARGED ENGINES - The demand for higher low engine speed torque is the driving force for expanding both turbine and compressor operating range; the low engine speed is equivalent to low mass flows and the desire for high torque sets the demand for high pressure ratios. The maximum turbo speed is a severe limitation at higher mass flows in the choke region of the compressor, which reduces the possibility of resizing the compressor to fit the low end

characteristics that are required. When compensating for high altitude as seen in Figure 1, it is clear that it is not a viable solution to select a smaller size of the compressor to avoid surge.

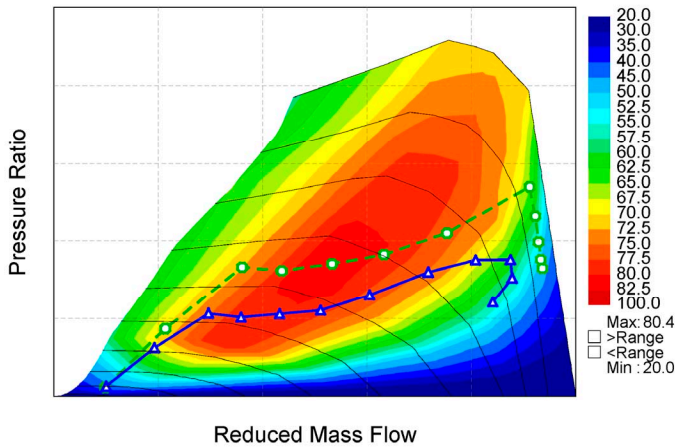


Figure 1 Simulated full load average operating points at sea level (solid line) and at high altitude (dashed line) for a waste-gate controlled SI engine.

Mild surge is accompanied by noise which is disturbing. Heavy surge, on the other hand, can cause significant loss of engine power and severe drivability issues. On waste gate controlled spark ignited engines; surge is most likely to occur during gear shifting and rapid throttle closing, when the engine air flow decreases rapidly, or at high altitude. CI or SI engines with variable turbine geometry for boost control are able to drive the compressor into surge by increasing the turbine power. The boost pressure has to be controlled to avoid surge for all these applications which requires a definition of a surge limit. The margin to surge that has to be maintained depends on the installation, controller authority and application. For example, a parallel twin turbo installation will probably need a larger margin to surge since the two compressors sometimes diverge to different operating points due to asymmetries in the engine piping.

There are significant differences in behavior between radial compressors that are run on test stands and those run on engine. Reciprocating internal combustion engines generate pulses in the intake system during the intake stroke. The operating point in the compressor varies during an engine cycle due to these pulsations, i.e. the average operating point in the compressor does not correspond to the actual time resolved operating points. The simulations in Figure 2 indicate that the magnitude of oscillation depend on the slope of the compressor speed lines. Evans and Ward [3] also discuss cyclic operating envelopes and the dependence of surge noise on the slope of compressor speed lines. Watson and Janota [2] discuss how inlet system pulsations influence the required margin to the surge line. A 10% margin in mass flow to the surge line is suggested in general and 20% for engines with low

number of cylinders. The required margin is also affected by potential resonances in the intake system which can be seen by comparing the cyclic operating envelopes in Figure 2 and Figure 3.

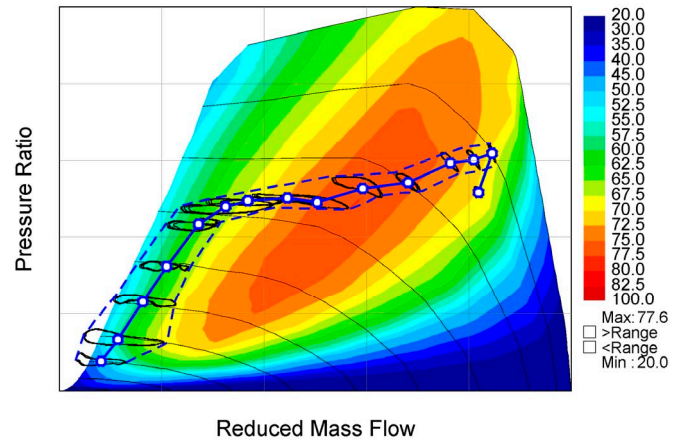


Figure 2 Average and cyclic simulated operating points at full load for a waste-gate controlled four cylinder SI engine.

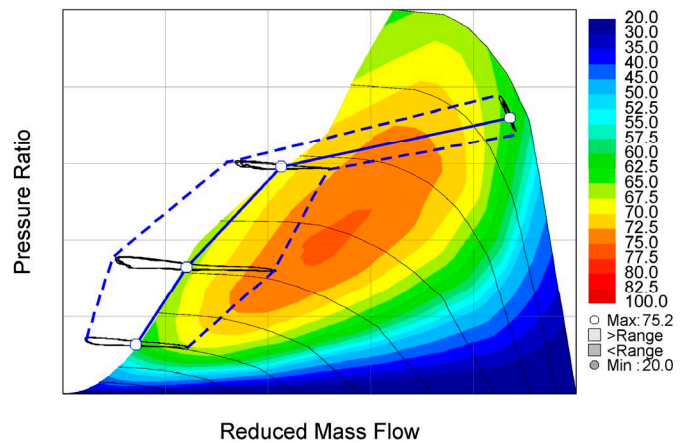


Figure 3 Average and cyclic simulated operating points at full load for a four cylinder CI engine with variable turbine geometry for boost control.

EXISTING STANDARDS OF MAP MEASUREMENT - SAE standards on turbo nomenclature and measurements [4][5] characterizes surge as severe flow reversal combined with audible coughing and banging and note that surge limits may vary from one installation to another. SAE J1723 [6] characterizes surge for non-positive displacement superchargers (e.g. centrifugal compressors) as severe air flow reversal with a sharp increase in inlet temperature and rapid pressure fluctuations. Inlet temperature is measured 2-3 pipe diameters upstream of the compressor inlet transition in [6].

The ASME standard for compressor measurement [7] is a measurement standard for performance characterization of compressors in general with high attention to inlet and outlet system geometries and instrumentation in static conditions. The dynamic characteristic of surge in automotive compressors is not considered. It is noted that the

installation will influence the surge line. The identified symptoms of surge are noise, mass flow fluctuations, a drop in pressure ratio and outlet temperature or outlet pressure and temperature fluctuations.

None of these standards give an objective or quantified way of defining surge or measuring centrifugal compressors close to surge. Figure 4 shows an example of two different surge definitions applied in gas stand testing of a compressor.

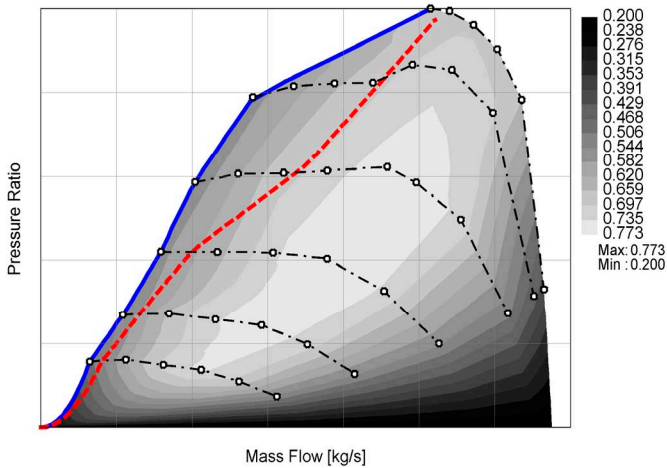


Figure 4 Two different surge definitions applied on a centrifugal compressor in steady flow testing. Complete system instability (solid line) and operator perceived noise (dashed).

OTHER WORKS ON COMPRESSOR SURGE MEASUREMENT - In descriptions of gas stand measurements of turbochargers, several techniques of detecting surge can be found. In [8] a fast pressure sensor on the compressor outlet is used. Galindo et. al. [9] advocates using pressure fluctuation amplitude obtained through FFT in the 5-15 Hz range as an objective indication of surge. Another way to detect surge is to observe the turbo speed variations that arise during deep surge. Subjective means of detecting surge include test operator perception of surge noise, which is perhaps the most relevant definition in order to avoid disturbing noise in a vehicle installation.

Pampreen [10] summarizes measurements and findings from many researchers and state that large amplitude pressure pulsations precede stall in the impeller or the diffuser which is not the case for inducer stall. Inducer stall and flow recirculation creates a positive prewhirl, which further deteriorates the inlet air flow angle relative to the impeller blades and creates more or larger stall regions, and also results in a temperature rise in the inlet up to 25 K according to [1] and more than 50 K according to [10].

MEASUREMENT SETUP

The main part of the experimental work has been conducted in a rig specifically designed for compressor studies. The rig is powered by an electrical motor that

drives a gear on which there is a centrifugal compressor of the same type as a conventional automotive turbocharger compressor. There are instrumented pipes upstream and downstream of the compressor for temperature, pressure and mass flow measurements. Pictures of the test rig can be seen in Figure 5.

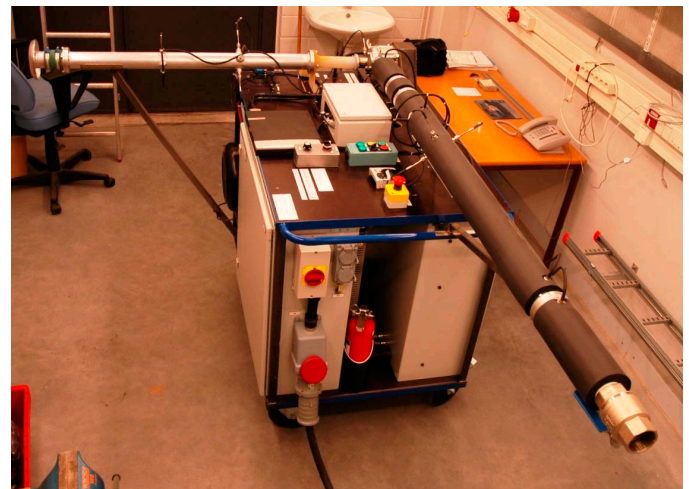
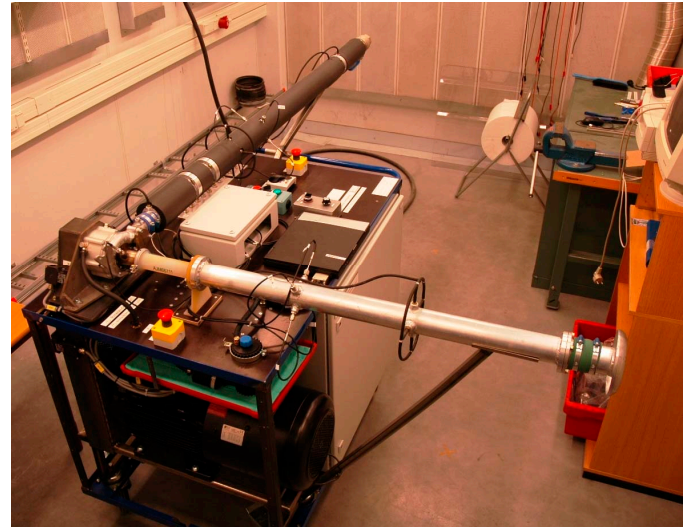


Figure 5 Pictures of the test rig used for experiments

The pressure ratio and mass flow of the compressor is controlled by a simple ball valve upstream of the compressor. The measurement pipes have standardized flanges for mounting of various devices such as Prandtl tube, pulse valve, extra volumes etc. The pipes downstream of the compressor have been thermally insulated up to the discharging valve in order to reduce errors due to heat losses. The compressor cover is however not insulated. In order to minimize rotational flow before and after the compressor, flow straighteners of the multitube/honeycomb type have been used. All the requirements in ASME Performance Test Code on Compressors and Exhausters [7] have been fulfilled.

Due to the fact that the electrical motor is speed controlled, the test method is very simple. Desired compressor speed is selected and pressure ratio as well

as mass flow is adjusted with the discharge valve after the compressor. Each speedline is measured from choke to surge by adjusting the discharge valve and waiting for the temperatures to stabilize before sampling of all relevant measurement signals.

There might be a slight impact on the surge behavior in this test rig compared to a complete turbo test rig since the electric motor is speed controlled. The compressor speed usually fluctuates by up to 3-4% during surge in a turbocharger [9].

COMPRESSOR AND GEAR SPECIFICATIONS - Two compressors have been tested on the test rig. Specifications are shown in Table 1.

Table 1 Specification of the compressors used during testing.

	Small compressor	Large compressor
Exducer diameter	52 mm	73 mm
Trim	55	43
Diffuser width	2.79 mm	4.5 mm
Maximum PR	2.7	2.8
Maximum mass flow	0.19 kg/s	0.27 kg/s

The compressor is mounted on a gear with 1:9.49 gear ratio. The belt drive from motor to gear pulley has a ratio of 1:3 which result in a total ratio of 1:28.47. The maximum impeller speed that can be obtained is nearly 160.000 rpm with this gear ratio, but due to slip inside the gear and in the belt drive the actual maximum speed is approximately 155.000 rpm. In the case of the larger compressor the maximum speed is however limited by the maximum power of the electrical motor; this reduces the available speed in which to obtain a complete speed line to 100.000 rpm with that compressor.

PULSE GENERATOR – To replicate the operating conditions of a compressor on an engine, a pulse generator in the shape of a speed controlled rotating butterfly valve was mounted on the outlet piping of the compressor. The pulse valve was designed to replicate a 2.0 litre in-line four cylinder engine with the projected opening area of the pulse valve approximately equal to the instantaneous overlapping inlet valve opening area of all four cylinders. This produces engine intake system like pulses, given that there is an adequately small volume between the pulse valve and the discharge valve, mounted in series downstream of the pulse valve.

TEMPERATURE AND PRESSURE MEASUREMENT - The air temperature measurements (before and after compressor) was measured with 3 mm Pt100 sensors with multiple sensors at each measurement station in accordance with ASME PTC10 [7], which define the minimum pipe lengths and general installation considerations. Apart from the standard inlet temperature sensors, a 2,2 mm Pt100 sensor was mounted in the

inducer of the compressor; two millimeters from impeller inlet axially and in the middle between hub and shroud radially, as shown in Figure 6. The intent of this sensor is to measure the temperature rise in the compressor inlet due to flow recirculation. The standard compressor inlet temperature is subtracted from the measured inducer temperature in order to define the temperature increase.

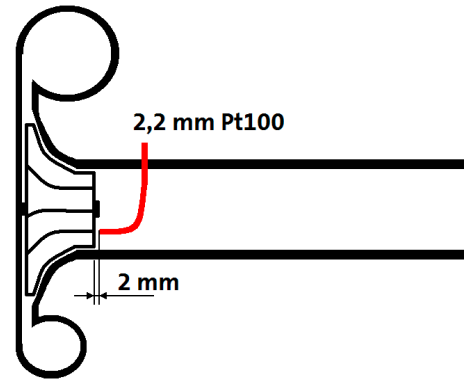


Figure 6 Baseline compressor inlet temperature instrumentation to measure temperature rise during surge.

To be able to check the axial temperature gradient in the compressor inlet pipe, an array of temperature sensors were mounted according to Figure 7. All sensor tips were located on approximately half the pipe radius from the pipe wall to avoid excessive heat transfer to and from the pipe wall. The orientation of the sensors towards the compressor wheel was chosen in order to capture the reversing warm flow close to surge in the best possible manner.

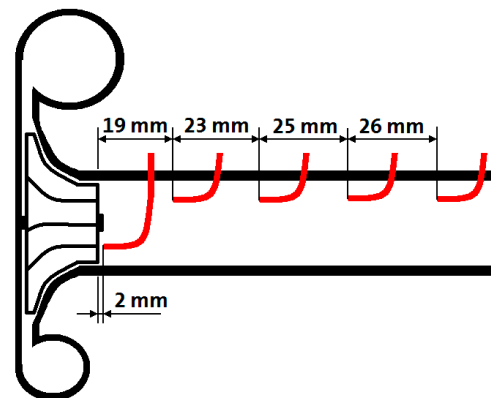


Figure 7 Temperature sensor locations for axial temperature gradient measurements.

A type K thermocouple with a 0.25 mm exposed measurement tip was also used to measure the radial temperature gradient in the compressor inlet.

Static pressure measurements are done by taps with 2 mm holes drilled radially into the pipe. The installation is in accordance with ASME PTC10 [7]. All pressure transducer signals have been filtered with 150 Hz analogue low pass filters prior to sampling with 300 Hz. The pressure after compressor, installed as specified in ASME PTC10 [7], is

also the basis for the standard deviation and FFT analysis as described in later sections.

MASS FLOW MEASUREMENT - Mass flow measurement and computation is based on the differential pressure over an orifice plate according to ISO 5167-1 [11]. The standard provides a number of design considerations which needs to be fulfilled such as surface finish, concentricity etc. These dimensions have all been verified to be within specification through measurements. A range of orifice plates had to be used to cover the complete mass flow range of a turbocharger compressor.

Calculation of mass flow is performed offline after testing according to the correlations found in [11]. In order to reduce the uncertainty of the results, the actual location of the pressure taps relative to the orifice plate upstream surface were measured as well as the actual diameter of the orifice plates that were manufactured. Thermal expansion of the steel plate and the aluminum pipes was taken into account by assuming that the insulated orifice plate and pipes have the compressor outlet temperature which is measured upstream of the orifice plate. All measured data were filtered with a zero phase shift digital low pass FIR-filter with adjustable cut-off frequency prior to the calculations. The mass flow was calculated from the time resolved pressure signals before averaging the mass flow in order to avoid distortions of the calculated mass flow due to nonlinearities in the expressions from ISO 5167-1 [11] as described in [12] and explained further below.

The ISO standard [11] also states how to estimate the uncertainty of the measured mass flow. The major contributors to the total uncertainty are the measured pressure drop over the orifice plate and the uncertainty in the expansion factor ϵ . With adequate selection of orifice diameter, the total uncertainty in measured mass flow was kept below 1%.

A HFM meter was used during the experiments with pulsating flow. The HFM was calibrated using the orifice plates, under steady state conditions down to 0.016 kg/s. The HFM used is not capable of measuring negative mass flow which means that no conclusions can be drawn regarding the reversed flow during surge. The location of the HFM is approximately 1500 mm upstream of the compressor unit.

MASS FLOW COMPUTATION IN PULSATING FLOW -

The orifice flow meter standard [11] state that the measurement method is only valid for steady flow. Compressor surge can cause an oscillating mass flow. Gajan et. al. [12] state that the flow can be regarded as steady if the velocity amplitude ratio is less than 0.05:

$$\frac{U_{rms}}{\bar{U}} < 0.05 \Rightarrow \text{steady flow} \quad \text{Eqn 1}$$

When the velocity amplitude ratio is less than 0.2, the differential pressure amplitude ratio is approximately twice the velocity amplitude ratio. If the velocity ratio is below 0.2 and the Strouhal number is less than 0.02, then the time average of the square root differential pressure will yield accurate estimates of time average flow rate, provided that the time resolved differential pressure is measured in an adequate way:

$$\left. \begin{aligned} \frac{U_{rms}}{\bar{U}} = \frac{1}{2} \frac{\Delta p_{rms}}{\Delta p_{avg}} < 0.2 \\ St = \frac{fd}{\bar{U}} < 0.02 \end{aligned} \right\} \Rightarrow \bar{Q}_m \propto (\sqrt{\Delta p})_{avg} \quad \text{Eqn 2}$$

Where f is the pulsation frequency, d is the orifice diameter, U is flow velocity, p is pressure and Q_m is mass flow. If the velocity ratio is greater than 0.2, the effects of pulsatile flow can not be neglected, i.e:

$$\frac{U_{rms}}{\bar{U}} > 0.2 \Rightarrow Q_m \text{ not well defined} \quad \text{Eqn 3}$$

The work in [12] mainly concerns the error in measured average flow. Some corrections to instantaneous flow rate from instantaneous differential pressure are also discussed. The formulas above can be used to check whether the measured mass flow is accurate in a test when the compressor is running at surge.

The surge operating points shown in this paper fall into the second category described above, i.e. the flow is unsteady but the average flow rate based on time resolved measurements and calculations are accurate. This was also confirmed through 3D CFD calculation of the orifice flow meter with surge-like pulsating flow. The time resolved pulsation amplitude is however underestimated in pulsating flow and the distance between the pressure transducers in the pipes cause some hysteresis. The CFD study was performed with 50 Hz pulse frequency, which is high compared to average surge cycles, and the error in mass flow due to pulsations was below 2% of the measured value.

COMPRESSOR PERFORMANCE PARAMETERS -

Total to total isentropic efficiency is calculated through temperature rise and pressure ratio over the compressor [4]. The average ratio of specific heats between inlet and outlet conditions was used in the calculations:

$$\eta_{C,t} = \frac{T_{1t} \cdot \left(\left(\frac{p_{2t}}{p_{1t}} \right)^{\frac{\kappa-1}{\kappa}} - 1 \right)}{(T_{2t} - T_{1t})} \quad \text{Eqn 4}$$

The uncertainty of calculated efficiency based on known inaccuracies in the measurement setup has been computed for two speedlines, 80 and 100 krpm. The

error is typically in the range of 2-3% of the calculated value. The maximum errors can be found in the choke region of each speedline.

The mass flow and compressor speed is corrected to 100 kPa and 298 K in accordance to [4] and [5]:

$$\dot{m}_{corr} = \frac{m_{meas} \cdot \sqrt{T_1/T_{ref}}}{P_1/P_{ref}} \quad \text{Eqn 5}$$

$$N_{corr} = \frac{N_{meas}}{\sqrt{T_1/T_{ref}}} \quad \text{Eqn 6}$$

CORRELATION TO OTHER TEST RIGS - In order to benchmark and validate the rig and measurement setup itself, the baseline data using the small compressor was compared to gas stand data from an independent turbocharger test facility. The result for pressure ratio versus mass flow can be seen in Figure 7. The calculated efficiencies obtained from the different test facilities are difficult to compare due to different heat transfer situations. The compressor used in this work has an oil cooled gear behind the compressor backplate, whereas the turbocharger tests were performed with a several hundred degrees warmer turbine on the other end of the turbo shaft. Overall, the efficiencies measured on the rig is approximately 5% lower than data from gas stand tests.

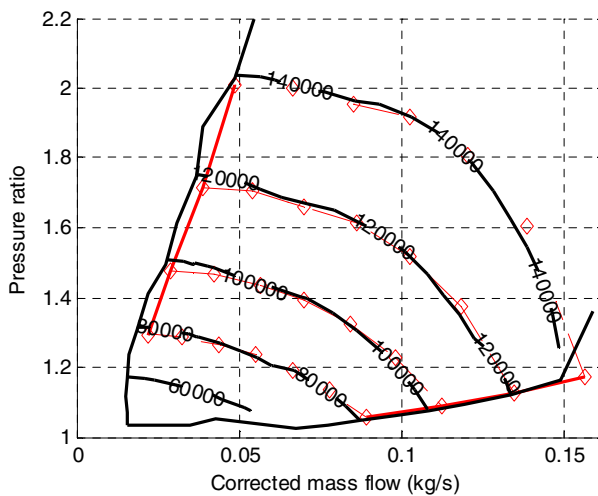


Figure 7 Compressor map comparison for the small compressor. Red lines with markers is reference data, black solid lines is rig data for the same compressor.

TEST RESULTS

OVERVIEW - It is clear from Figure 7 that there is a good correlation between rig test results and gas stand test data. Following the baseline test a study of different surge indicators was performed for both compressors.

The temperature gradient in the compressor inlet has been characterized in order to find guidelines for instrumentation. The influence of the piping surrounding the compressor and pulsating flow has also been studied to verify that the surge indicators are valid for a wide range of test conditions including gas stand testing. Finally, a series of car tests were performed to make a correlation between easily measurable surge indications to perceived noise in a vehicle.

TIME RESOLVED MEASUREMENT OF SURGE – Figure 8 and Figure 9 shows time resolved measurements of steady operating points and operating points in heavy surge with complete flow reversal. The pressurized volume after the compressor is approximately 4.8 dm³ which causes a significant damping of the mass flow fluctuations that occur in the compressor. The signal measured with the HFM exhibits the characteristic features of a surge cycle with flow reversal near constant pressure, an increasing mass flow at lower pressure, a rapid increase of mass flow back to a steady flow compressor speed line and finally pressure build up to the starting point on the surge limit. Since the inlet air is heated by the reversed flow, the restoration of the pressure initially occurs at a lower corrected compressor speed and higher corrected mass flow. Furthermore, the backflow of the compressor will have an axial swirl generated by the impeller itself increasing the map size. The frequency of the surge cycle depends on the compressor speed and system volumes and was found to be in the 5-15 Hz range as described in [9].

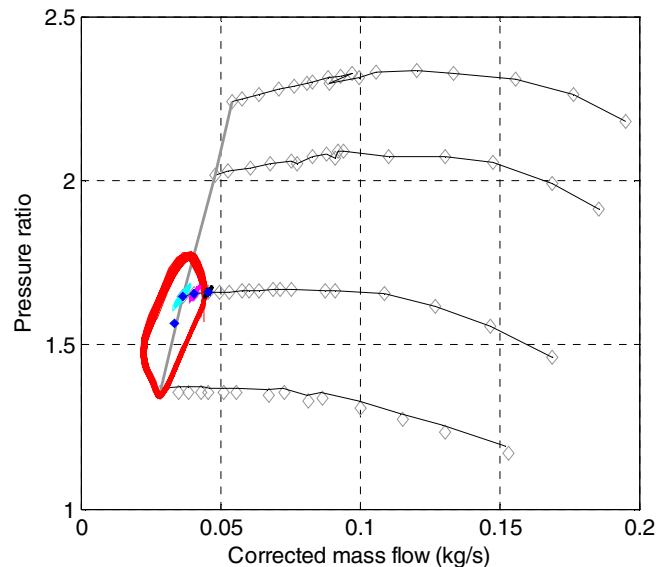


Figure 8 Example of time resolve surge loops measured with orifice flange at outlet of compressor. Blue diamonds indicate averaged operating points.

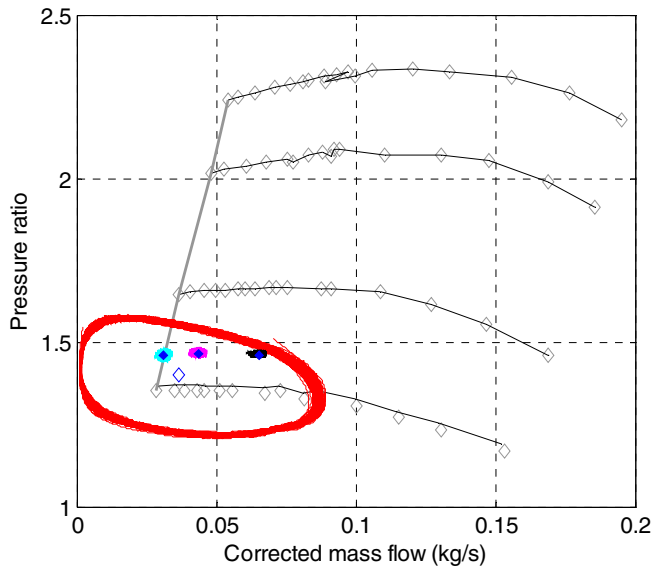


Figure 9 Example of time resolve surge loops measured with HFM at inlet of compressor. Blue diamonds indicate averaged operating points. The averaged operating point for surge using the HFM can however not be seen as valid due to lack of HFM calibration in massflows < 0,016 kg/s.

It should be noted that the average pressure ratio vs. mass flow point is irrelevant when the compressor runs in surge since there is no stable operating point corresponding to that time average mass flow and pressure ratio. The average surge point should not be confused with extended compressor maps used for surge simulation described in for example [13].

The difference in mass flow oscillations measured with HFM and orifice plates is caused by the orifice plates being placed downstream of the compressor, while the HFM is placed upstream. This in turn leads to compression/expansion effects with pressure fluctuations on the downstream side of the compressor, i.e. since the backflow is being tapped from the bulk of high pressure air downstream of the compressor the result is smaller mass flow oscillations through the orifice plate. On the upstream side where the HFM is mounted the compression/expansion effect is however negligible.

SURGE INDICATORS ON SMALL COMPRESSOR - The inducer air temperature was measured in the entire compressor map of the small compressor and compared to the inlet temperature. The standard deviation of the time resolved (300 Hz) pressure after compressor, σ_{p2} , was also analyzed. These indicators have been plotted into the compressor map in Figure 10 and Figure 11. Both these maps were measured all the way to where the pressure build-up collapses completely, i.e. to heavy surge.

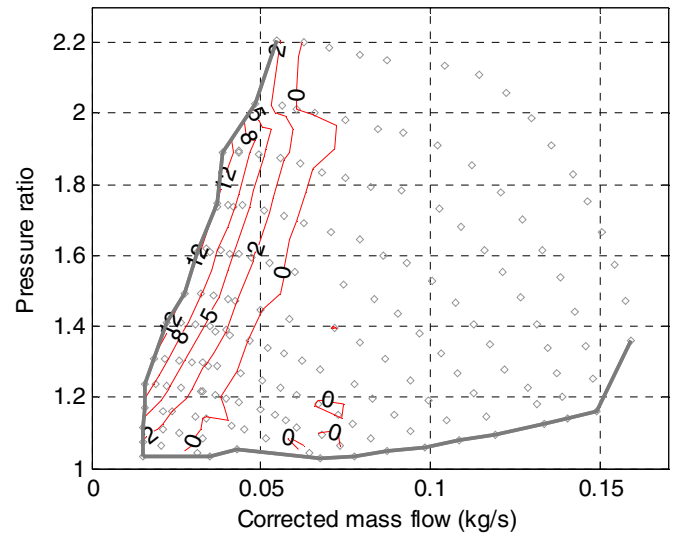


Figure 10 Inducer temperature rise plotted in compressor map of the small compressor.

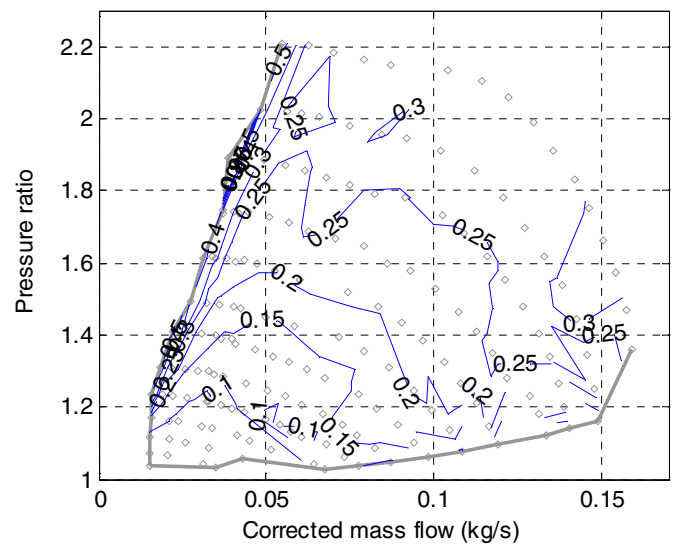


Figure 11 Standard deviation of time resolved post compressor pressure plotted in the map of the small compressor.

The temperature gradient in Figure 10 indicates partial backflow into the inducer of the compressor even when there is a margin to heavy surge. This behavior can be useful if NVH limits prior to fully developed surge are to be introduced. A drawback of the inlet temperature rise as a surge indicator, at least for this specific compressor, could be that the gradient is much steeper at higher pressure ratios where disturbing noises are most likely to occur, according to the literature [3] and as clearly visible in Figure 4.

The standard deviation of the pressure after compressor, σ_{p2} , exhibits a much steeper gradient close to heavy surge than the inducer temperature. The general signal noise level increases for higher mass flows and pressure ratios which cause σ_{p2} to rise, but the pressure oscillations close to surge are still clearly visible.

SURGE INDICATORS ON LARGE COMPRESSOR –
 Due to the power limitations in the electric motor, only part of the large compressor map could be measured with the two surge indicators. Figure 12 and Figure 13 show the results of these measurements. The plotted surge limit is the point of complete flow reversal as before.

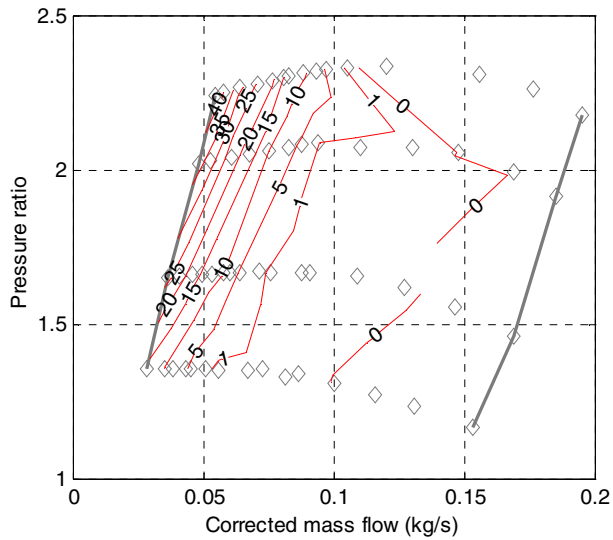


Figure 12 Inlet temperature rise in a part of the large compressor map close to surge.

temperature iso-lines are not as parallel to the surge limit as for the small compressor. To summarize, the inlet temperature rise gives an indication of surge for the large compressor, but it is difficult to correlate surge to an exact temperature rise.

The large compressor has quite different characteristics from the smaller compressor, with speed lines that have positive slope. As stated in several publications [3][1], the positive slope is a hint that there is local stall or flow reversal somewhere in the compressor which might result in noise problems. This is also evident from the σ_{p_2} data in Figure 13 which has a clear increase in the region around the peak of the highest speed lines. There was also a clearly audible noise from the compressor at these operating points.

Galindo et. al. [9] suggests using the maximum amplitude in the 5-15 Hz range of the Fourier transform (FFT) of compressor outlet pressure as a robust and objective measure of surge. This has been tested for the large compressor and compared to standard deviation data in Figure 14. The FFT-method is less sensitive to signal noise and the values are consistently lower than the standard deviation at low amplitudes when there is no surge. The much simpler calculation of the standard deviation does however produce very similar results at larger oscillation amplitudes.

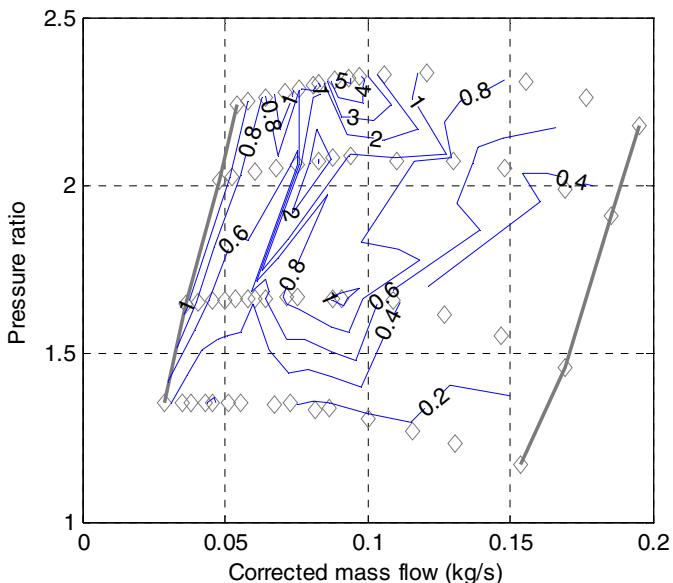


Figure 13 Standard deviation of time resolved compressor outlet pressure for the large compressor.

The temperature gradient is smooth close to surge also for this compressor. The inlet temperature rise is higher for the larger compressor than the smaller compressor, 20-40 K for the large compressor versus approximately 10-12 K at heavy surge in the small compressor. The

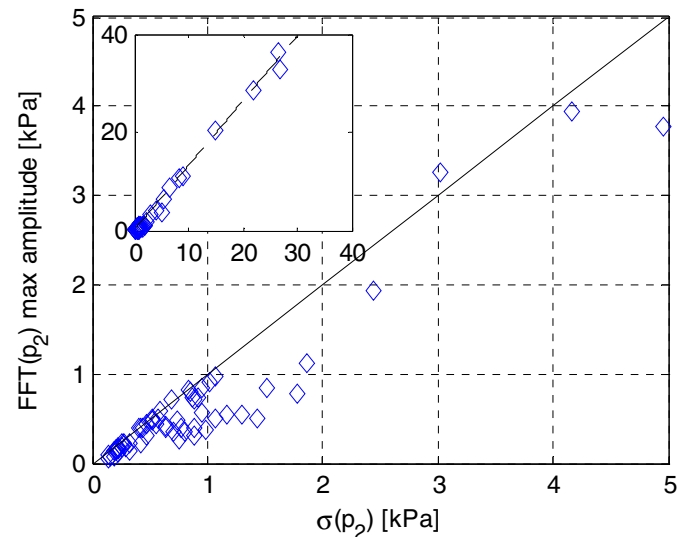


Figure 14 Comparison of standard deviation σ_{p_2} and max FFT amplitude of compressor outlet pressure sampled at 300 Hz for an entire compressor map.

INDUCER TEMPERATURE SENSOR LOCATION – The sensitivity of inducer temperature rise measurements to sensor location was examined for the large compressor. Figure 15 shows the axial temperature distribution together with the baseline inducer temperature installation as described in Figure 7 for several mass flows close to heavy surge at 80 krpm. The sensor pipe was also rotated 180° to check the radial homogeneity of the inducer temperature.

The sensors that are closer to the impeller exhibit a higher temperature rise and also start to indicate flow recirculation further away from surge than the sensors mounted upstream. The sensor 19 mm upstream of the impeller consistently shows higher temperatures than the baseline sensor 2 mm from the impeller. The radial temperature distribution is largest close to the compressor and it has almost disappeared completely 97 mm upstream of the impeller. It has to be concluded that the axial sensor location will influence the level and smoothness of the temperature gradient in the compressor map.

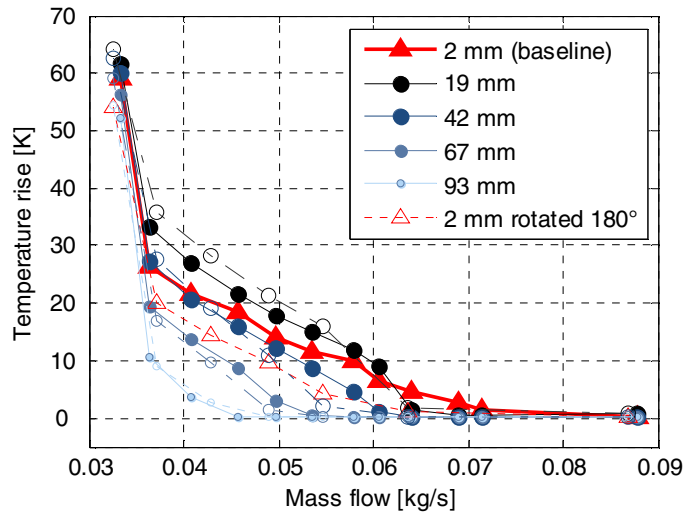


Figure 15 Axial temperature distribution in the inducer at 80 krpm on the large compressor. Dashed lines representing sensors rotated 180° in relation to solid lines.

The radial temperature distribution in the inducer is shown in Figure 16. This temperature was measured with the 0.25 mm exposed tip thermocouple to minimize the space averaging of an ordinary sheathed temperature probe. Another reason for using this probe instead of previously used Pt100 sensors is that the error of heat transfer between the sensor and pipe wall is minimized, which is critical when the sensor protrude very little into the air flow. The probe was traversed in steps of 5 mm, from the outer diameter of the inducer to the hub of the impeller. This was performed at both the axial distance of 2 mm as well as 20 mm from the impeller.

It is clear that there is more backflow at the outer diameter of the inducer. This corresponds well with the compressor surge backflow distribution described in [1]. A steeper and clearer temperature gradient might be achieved by choosing to measure the surge temperature gradient at the outer diameter; however the need to eliminate the effect of thermal conduction to the probe does present a problem.

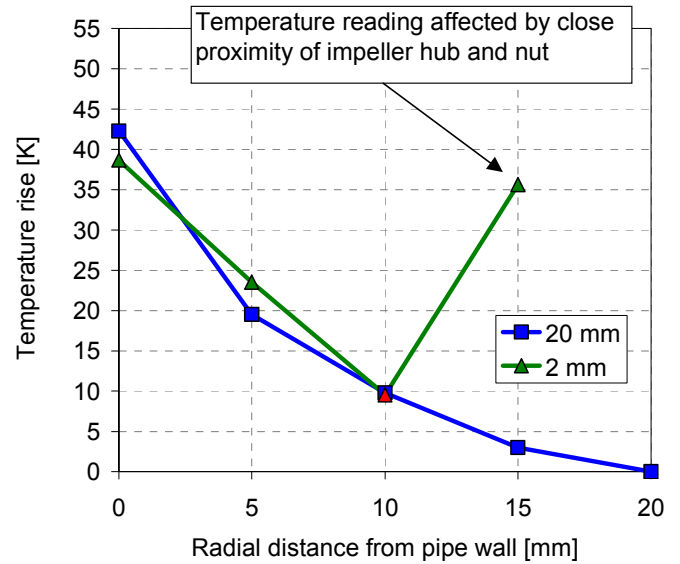


Figure 16 Radial temperature distribution in the inducer measured with 0.25 mm thermocouple with exposed probe tip. Large compressor operating close to surge.

SURGE INDICATORS IN PULSATING FLOW - Tests were also performed in pulsating flow with pulses similar to a four cylinder engine at 2000 and 1500 rpm. The mass flow fluctuations for the 2000 rpm pulse trace are shown in the compressor map of the large compressor in Figure 17.

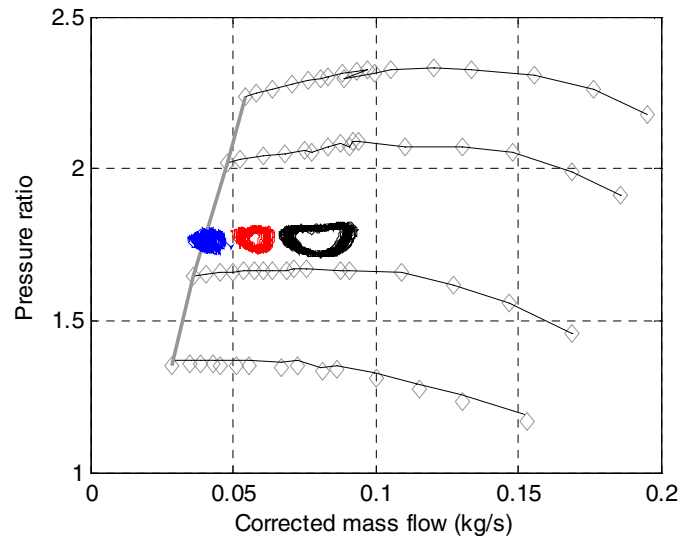


Figure 17 Mass flow oscillations in pulsating flow similar to operation at 2000 rpm on a 4-cylinder engine. Measured data using large compressor.

The inducer temperature rise measured in pulsating flow is very similar to steady flow measurements as shown in Figure 18. This indicates that the inducer temperature rise should be a good indicator of proximity to surge also when the compressor is mounted on an engine.

Higher pulse frequency gives an inducer temperature rise further away from surge than with steady flow. An explanation to this could be that the mass flow pulse amplitude of the pulse generator increases as the discharge valve is opened and this is not an engine-like behavior. However, this should not impair the ability to draw conclusions regarding surge indicators in pulsating flow.

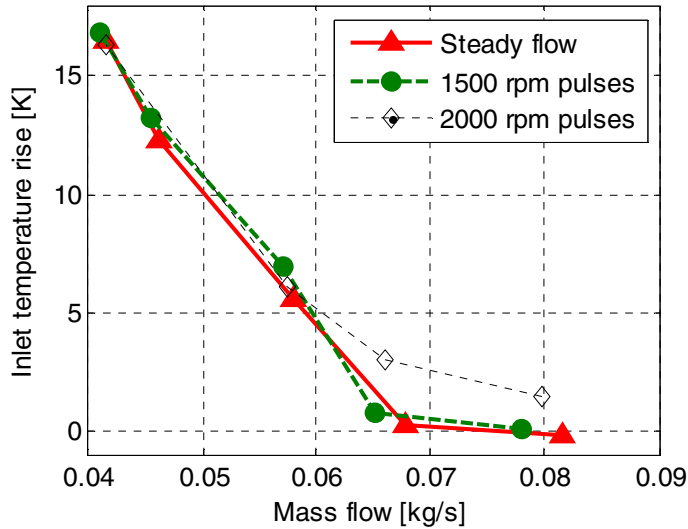


Figure 18 Compressor inlet temperature rise measured with steady flow and pulsating flow with pulse frequency and amplitude similar to a 4 cylinder engine. Large compressor at 90 kprm.

Figure 19 shows the calculated standard deviation of the compressor outlet pressure in pulsating flow compared to the steady flow measurements. The generated pulses make it impossible to see the pressure oscillations due to mild surge in the simple standard deviation values. The Fourier transform method from [9] obviously gives a much better result under pulsating conditions. In this case the maximum amplitude was searched in the 0-20 Hz range.

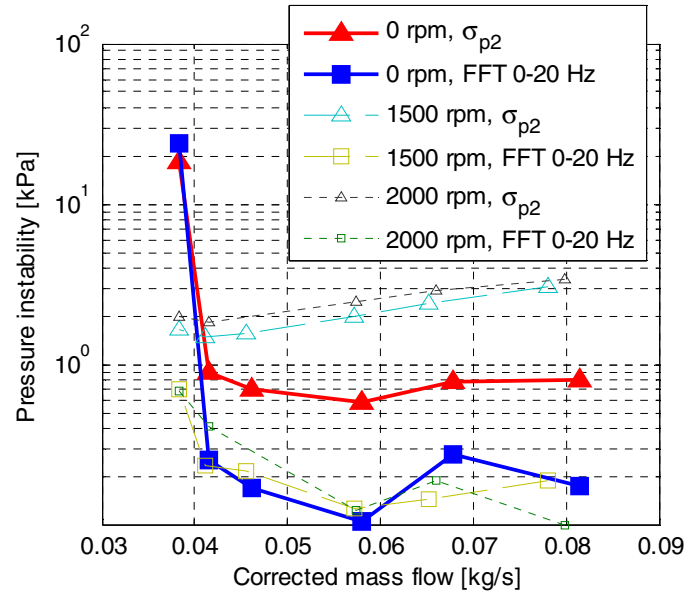


Figure 19 Standard deviation of compressor σ_{p2} outlet pressure and max amplitude of FFT. Large compressor in operation close to surge in steady and pulsating flow.

EFFECT OF INLET BENDS – In order to investigate the robustness of the method of measuring the inducer temperature rise a minor study with severe inlet bends has also been conducted. Two 90° bends with different temperature probe positions has been tested. The results are shown in Figure 20.

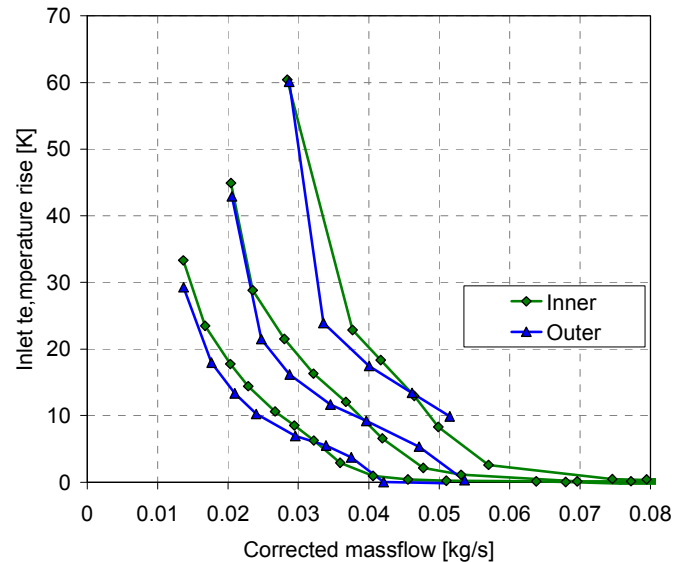


Figure 20 Compressor inlet temperature rise with 90° inlet bend at three different compressor speeds. Temperature probe inserted in both outer and inner radius of bend. Data acquired using the small compressor.

It is clear that the temperature rise indication is valid for sharp inlet bends, in this case 90° bends that can be considered to be worst case packaging scenarios with regards to inlet flow distribution of the compressor. The levels of temperature rise do however differ between the

two sensor positions, which mean that a generic level of temperature rise cannot be defined as a surge limit.

GAS STAND TESTS - A compressor in similar size to the small compressor used in the test rig was measured in a gas stand. A temperature sensor in the inducer, 5 mm from impeller, was installed as well as a fast pressure transducer that measured pressure after the compressor. In Figure 21 the inducer temperature rise is plotted in the compressor map and it is clear that the temperature gradient close to the surge limit can be measured in the same manner as on the test rig. It can also be observed from the figure that the steepness of the inducer temperature rise is noticeably more severe at higher pressure ratios; similar results have been evident in the tests from the smaller compressor as seen in Figure 10. The large compressor does not exhibit the same behavior however; this can be attributed to the different inducer design of that compressor.

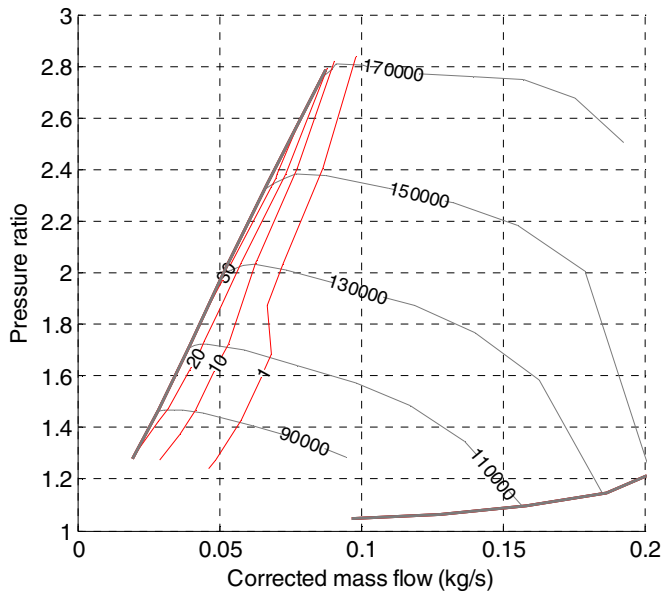


Figure 21 Inducer temperature rise for a compressor tested at gas stand.

The pressure fluctuations at compressor outlet have also been logged and the result is shown in Figure 22.

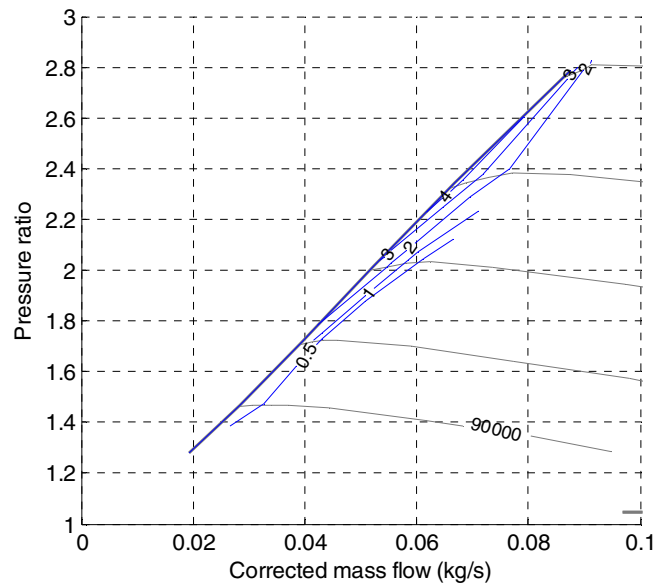


Figure 22 Standard deviation of time resolved compressor outlet pressure for a compressor tested on gas stand.

Again, it is clear that an analysis of the compressor outlet pressure can be used for surge detection. The method is however more complex since time resolved logging equipment and post processing of data is necessary, furthermore the width of the gradient is also slightly less when compared to the inducer temperature rise.

CAR TESTS - The vehicle used was a SAAB 9-3 Sedan, with a 2.0 liter transversally mounted in-line 4 cylinder SI engine. The turbocharger is mounted on the fire-wall side of the engine, i.e. between the engine and the passenger compartment. The air filter box and all upstream compressor piping is plastic, the downstream compressor pipe before charge air cooler is made of metal and downstream the charge air cooler the piping is made of rubber. In order to supply enough power to the compressor as to facilitate fully developed surge the standard fixed geometry turbocharger has been replaced with a turbocharger with a variable turbine. No other modifications have been done in the vehicle.

The measurement setup is significantly simplified in comparison with the test rig:

- Pt100 temperature sensors were placed in the air filter box as well as in the inducer of the compressor (2 mm from impeller, as in Figure 6)
- Pressure sensors were installed pre and post compressor
- Turbine speed sensor was installed
- Mass flow was sampled via the HFM used by the engine control system

Two types of investigations were performed with the vehicle:

- Steady state mapping of compressor inlet temperature levels on chassis dyno
- Subjective noise testing when run on road. These tests were conducted with several people judging the sound level of the car from inside the passenger compartment

The vehicle was also equipped with a pushbutton which was logged together with the sensors in the measurement system. The button was used in the subjective grading of the sound level, i.e. for the driver to push the button at different sound levels. In this case 2 limits were selected: non-saleable sound level and the presence of high boost whistle noise. The temperature gradient acquired from chassis dyno testing is plotted on independent gas stand test data in Figure 23 together with non-saleable sound limit as blue diamonds. Due to power limitations in dyno as well as in engine durability considerations when running at high boost pressures the amount of compressor inlet temperature data is limited as is clear in Figure 23.

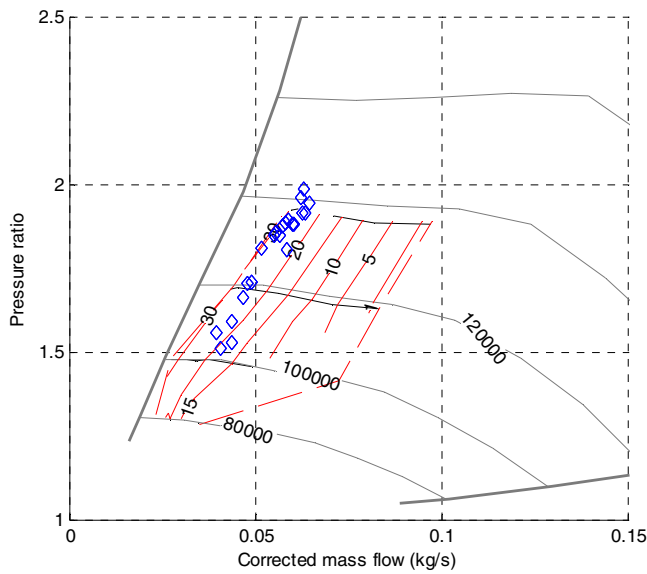


Figure 23 Subjective surge non-saleable limits as blue diamonds in compressor map with inducer temperature rise

It is clear that there is a correlation between inducer temperature rise and the noise limit experienced in the tested car. It is however important to bear in mind that the noise level is dependant on installation, sound proofing etc, which precludes the inducer temperature rise level at this specific noise limit from being valid for all vehicles and installations.

Pressure before and after the compressor was also evaluated from the noise limit test data acquired at vehicle tests on road. It became clear that the noise limit was evident long before any significant pressure oscillations could be detected in the FFT analysis of the pressure traces.

The noises encountered at the non-saleable level were predominately light roaring and rushing sounds. Another interesting sound was the whistling sound at higher boost pressures. Even though the sound was detected in a clearly non-saleable noise area in the compressor map in which the inducer temperature rise wasn't measured, it is interesting to mark the presence of such a distinctly different sound. The results can be seen in Figure 24.

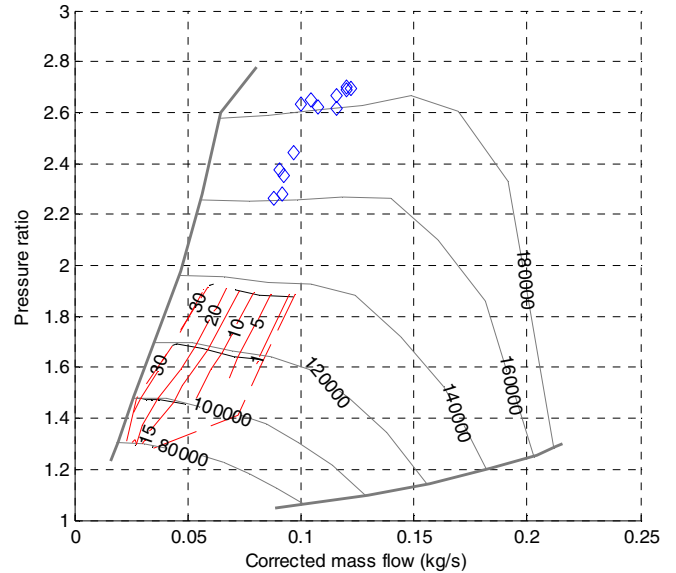


Figure 24 Subjective surge limits in compressor map with inducer temperature rise from road tests, blue diamonds indicate high boost whistle noise.

Finally, a comparison between independent gas stand testing, supplier data and subjective noise detection in car is presented in Figure 25.

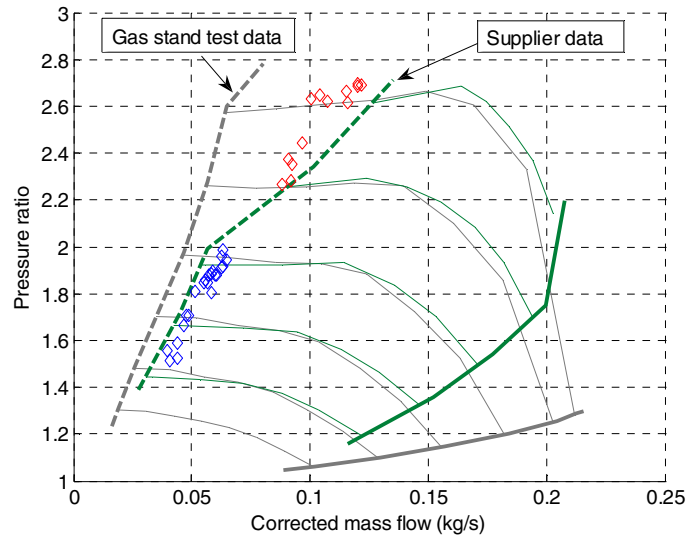


Figure 25 Subjective surge limits in compressor map, comparison with supplier data and gas stand test data for same compressor.

DISCUSSION

SURGE DEFINITIONS – It has been shown that the standard deviation of the time resolved compressor outlet pressure is a simple indicator of mild and heavy surge in steady flow. For pulsating flow, frequency analysis with Fourier transform has to be used [9]. For real engine measurements, even the FFT method seems difficult. In the ideal case, as with the pulse valve used in this work, each cylinder gives an identical pulse in the intake system and the frequency of the engine generated pulses exceeds the typical surge frequencies. On real engines, the pulses from each cylinder might be slightly different due to asymmetries in the piping. The lowest frequency content of such a pressure signal will be equivalent to half the engine speed, i.e. once per each four stroke cycle for a cylinder. This frequency might well be in the same range as typical surge frequencies on low engine speeds. For example, at 1200 rpm the lowest harmonic in the intake system could be at 10 Hz.

Different compressor behaviors and different boundary conditions such as skewed compressor inlet flow profiles result in different temperature rise gradients when approaching surge. This constitutes a problem when applying correlations between temperature rise and NVH limits as generic rules do not apply. This could perhaps be rectified by a larger study of different compressor characteristics and different boundary conditions. Even so, it could be the case that the outcome of such an investigation may be limited to “rules of thumb” rather than specific levels.

SIMULATION REQUIREMENTS ON COMPRESSOR MAP DATA – Compressor maps are sometimes truncated at the application specific surge limit. This limit applies to the average pressure ratio vs. mass flow operating points, which is not equivalent to the crank angle resolved operating traces on an engine as shown in Figure 2 and Figure 3. If the compressor map is truncated at the application specific average surge limit, the performance data to the left of the surge limit has to be guessed or extrapolated in order to perform crank angle resolved engine simulations. To be able to simulate the compressor in an adequate way, the compressor map data should be extended to, but not including, fully developed surge. Figure 8 shows the unsteady operation of a surging compressor, and the compressor map data represents steady flow performance data. The unsteady flow (surge) average operating point data in [5] is not relevant to the quasi steady approach commonly used to simulate compressors.

CONCLUSION

The results from the work regarding surge detection can be summarized in the following bullets:

- Inducer temperature rise can be used to indicate the surge margin under both steady and pulsating flow as well as with different inlet geometries to the compressor
- The measured inducer temperature rise is affected by the location of the sensor tip; however the characteristics of the temperature rise is maintained within a fairly large region in the inducer. Placement on half the inducer inlet radius up to 10 mm from the impeller is a reasonable compromise
- Inducer temperature rise values varies between different compressors, making generally valid correlations of temperature rise to surge limit difficult
- A simple evaluation of the standard deviation of the time resolved compressor outlet pressure signal can be considered as an alternative to the more elaborate FFT analysis proposed in [12], at least for steady flow operating points
- In pulsating flow the FFT analysis of the pressure oscillations after the compressor is necessary to detect surge
- Neither the standard deviation nor the FFT analysis of the compressor outlet pressure is applicable in engine testing due to low frequency oscillation induced by the engine
- There is a clear correlation between noise level in car and inducer temperature rise

4 different compressor designs have been used in the course of these investigations. Test results show that all these compressors can be measured and analyzed for surge margin using the measurement setup described above.

For engine simulation purposes it is essential to measure the entire compressor map down to, but not including, fully developed surge operating points. An application specific surge limit in the interior of the compressor map can of course be included in the data supplied for a compressor.

It is the hope of the authors that this work could lead to further standardization of automotive compressor map measurements. We suggest that at least one surge indicator should be included in the compressor map measurement standards for gas stand testing. The addition of one or several surge indicators in the compressor map data would enable an assessment of the surge margin of an operating point. It has to be agreed within the automotive community how to standardize the measurement and evaluation of this surge indicating data.

REFERENCES

1. Japiske, D., Baines, N. C.; Introduction to Turbomachinery; Concepts ETI, Inc. and Oxford University Press 1997; ISBN 0-933283-10-5
2. Watson, N., Janota, M. S.; Turbocharging the Internal Combustion Engine; The Macmillan Press Ltd, London, 1982; ISBN 0 333 24290 4
3. Evans, D., Ward, A.; Minimizing Turbocharger Whoosh Noise for Diesel Powertrains; SAE Technical Paper 2005-01-2485
4. Turbocharger Nomenclature and Terminology; Surface Vehicle Recommended Practice SAEJ922v001 Reaffirmed 1995-06
5. Turbocharger Gas Stand Test Code; Surface Vehicle Recommended Practice SAEJ1826v001 Reaffirmed 1995-03
6. Supercharger Testing Standard; Surface Vehicle Standard SAE J1723 Issued 1995-08
7. Performance Test Code on Compressors and Exhausters; The American Society of Mechanical Engineers standard ASME PTC 10-1997 issued Sept 30, 1998
8. Naundorf, D., Bolz, H, Mandel, M; Design and Implementation of a New Generation of Turbo Charger Test Bench Using Hot Gas Technology; SAE Technical Paper 2001-01-0279
9. Galindo, J., Serrano, J.R., Guardiola, S., Cervelló, C; Surge limit definition in a specific test bench for the characterization of automotive turbochargers; Experimental Thermal and Fluid Science 30 (2006) 449-462
10. Pampreen, R. C.; Compressor Surge and Stall; Concepts ETI, Inc., Norwich, Vermont 1993; ISBN 0-933283-05-9
11. International Standard ISO 5167-1:1991/Amd.1:1998(E)
12. Gajan, P. et. al.; The influence of pulsating flows on orifice plate flow meters; Flow Measurement and instrumentation, Vol. 3 Iss. 3 pp 118-129 (1992)
13. G. Theotokatos, N. P. Kyrtatos: Diesel Engine Transient Operation with Turbocharger Compressor Surging; SAE Technical Paper 2001-01-1241

CONTACT

Johannes Andersen, johannes.andersen@se.gm.com

Fredrik Lindström, fredrik.lindstrom@se.gm.com

Fredrik Westin, fredrik.westin@se.gm.com

DEFINITIONS, ACRONYMS, ABBREVIATIONS

NVH: Noise, Vibration and Harshness

Trim: Ratio between the outer and inner diameter of the

impeller: $Trim = \left[\frac{d^2}{D^2} \right] * 100$

FTT: Fast Fourier Transform

CFD: Computational Fluid Dynamics

CI: Compression ignited

HFM: Hot Film Meter

SI: Spark ignited

ASME: The American Society of Mechanical Engineers